

1 **Blowing Snow Sublimation and Transport over Antarctica from 11 Years of CALIPSO**
2 **Observations**

3 Stephen P Palm¹, Vinay Kayetha¹, Yuekui Yang² and Rebecca Pauly¹

4 ¹Science Systems Applications Inc., 10210 Greenbelt Road, Greenbelt, Maryland USA 20771.

5 ²NASA Goddard Space Flight Center, Greenbelt, Maryland USA 20771.

6

7 Address for all correspondence:

8 Stephen Palm, Code 612, NASA Goddard Space Flight Center, Greenbelt, Maryland USA 20771.

9 Email: stephen.p.palm@nasa.gov

10 Phone: +1-301-614-6276

11

12 **ABSTRACT**

13 Blowing snow processes commonly occur over the earth's ice sheets when the 10 m wind speed
14 exceeds a threshold value. These processes play a key role in the sublimation and re-
15 distribution of snow thereby influencing the surface mass balance. Prior field studies and
16 modeling results have shown the importance of blowing snow sublimation and transport on the
17 surface mass budget and hydrological cycle of high latitude regions. For the first time, we
18 present continent-wide estimates of blowing snow sublimation and transport over Antarctica
19 for the period 2006 - 2016 based on direct observation of blowing snow events. We use an
20 improved version of the blowing snow detection algorithm developed for previous work that
21 uses atmospheric backscatter measurements obtained from the CALIOP (Cloud-Aerosol Lidar
22 with Orthogonal Polarization) lidar aboard the CALIPSO (Cloud-Aerosol Lidar and Infrared
23 Pathfinder Satellite Observation) satellite. The blowing snow events identified by CALIPSO and
24 meteorological fields from MERRA-2 are used to compute the blowing snow sublimation and
25 transport rates. Our results show that maximum sublimation occurs along and slightly inland of
26 the coastline. This is contrary to the observed maximum blowing snow frequency which occurs
27 over the interior. The associated temperature and moisture re-analysis fields likely contribute
28 to the spatial distribution of the maximum sublimation values. However, the spatial pattern of
29 the sublimation rate over Antarctica is consistent with modeling studies and precipitation

30 estimates. Overall, our results show that the 2006 – 2016 Antarctica average integrated
31 blowing snow sublimation is about $393 \pm 196 \text{ Gt yr}^{-1}$ which is considerably larger than previous
32 model-derived estimates. We find maximum blowing snow transport amount of 5 Megatons
33 $\text{km}^{-1} \text{ yr}^{-1}$ over parts of East Antarctica and estimate that the average snow transport from
34 continent to ocean is about 3.7 Gt yr^{-1} . These continent-wide estimates are the first of their
35 kind and can be used to help model and constrain the surface-mass budget over Antarctica.

36

37 **Keywords:** Blowing snow, sublimation, transport, CALIPSO, Antarctica, surface mass balance

38

39 **1 Introduction**

40 The surface mass balance of the earth's great ice sheets that cover Antarctica and Greenland is
41 one of today's most important topics in climate science. The processes that contribute to the
42 mass balance of a snow or ice-covered surface are precipitation (P), surface evaporation and
43 sublimation (E), surface melt and runoff (M), blowing snow sublimation (Q_s) and snow transport
44 (Q_t). Sublimation of snow can occur at the surface but is greatly enhanced within the
45 atmospheric column of the blowing snow layer. The contributions of these processes to the
46 mass balance vary greatly spatially, and can be highly localized and very difficult to quantify.

$$47 \quad S = \int_{\text{year}} (P - E - M - Q_t - Q_s) dt \quad (1)$$

48 It is well known that the Arctic is experiencing rapid warming and loss of sea ice cover and
49 thickness. In the past few decades, the Arctic has seen an increase in average surface air
50 temperature by $2 \text{ }^\circ\text{C}$ (Przybylak, 2007). Modeling studies suggests an increase in annual mean
51 temperatures over the Arctic by $8.5 \pm 4.1 \text{ }^\circ\text{C}$ over the current century that could lead to a
52 decrease in sea ice cover by $49 \pm 18 \%$ (Bintanja and Krikken, 2016). While the Antarctic has
53 experienced an increase in average surface temperature, most of the warming is observed over
54 West Antarctica at a rate of $0.17 \text{ }^\circ\text{C}$ per decade from 1957 to 2006 (Steig et al., 2009; Bromwich
55 et al., 2013). Such surface warming undoubtedly has implications for ice sheet mass balance
56 and sea level rise mainly through the melting term of the mass balance equation. However, the
57 other processes affecting the mass balance of ice sheets may also be experiencing changes that

58 are difficult to identify and quantify. For instance, models have shown that in a warming
59 climate, precipitation should increase over Antarctica and most of it will fall as snow (Church et
60 al., 2013). If snowfall is increasing, perhaps the frequency of blowing snow and subsequently
61 the magnitude of transport and sublimation will increase as well. Thus, understanding how
62 these processes affect the overall mass balance of the ice sheets and how they may be
63 responding to a changing climate is of growing concern.

64 In addition to ice sheet mass balance, sublimation of blowing snow is also important for the
65 atmospheric moisture budget in high latitudes. For instance, in the Canadian Prairies and parts
66 of Alaska sublimation of blowing snow was shown to be equal to 30 % of annual snowfall
67 (Pomeroy et al., 1997). About 50 % of the wind-transported snow sublimates in the high plains
68 of southeastern Wyoming (Tabler et al., 1990). Adequate model representation of sublimation
69 processes are important to obtain reliable prediction of spring runoff and determine the spatial
70 distribution/variability of energy and water fluxes and their subsequent influence on
71 atmospheric circulation in high latitude regions (Bowling et al., 2004).

72 Over Antarctica, blowing snow occurs more frequently than anywhere else on earth. Models
73 driven by long-term surface observations over the Neumayer station (East Antarctica), estimate
74 that blowing snow sublimation removes up to 19 % of the solid precipitation (Van den Broeke
75 et al., 2010). Over certain parts of the Antarctica, where persistent katabatic winds prevail,
76 blowing snow sublimation is found to remove up to 85 % of the solid precipitation (Frezzotti et
77 al., 2002). Over coastal areas up to 35% of the precipitation may be removed by wind through
78 transport and sublimation (Bromwich 1988). Das et al., (2013) concluded that ~ 2.7–6.6 % of
79 the surface area of Antarctica has persistent negative net accumulation due to wind scour
80 (erosion and sublimation of snow). These studies show the potential role of the blowing snow
81 sublimation process in the surface mass balance of the earth's ice sheets.

82 For the current work, we focus on blowing snow processes over the Antarctic region. Due to the
83 uninhabited expanse of Antarctica and the lack of observations, prior, continent-wide studies of
84 blowing snow sublimation over Antarctica had to rely on parameterized methods that use
85 model re-analysis of wind speed and low level moisture. The presence of blowing snow is
86 inferred from surface temperature, wind speed and snow age (if known). In a series of papers

87 on the modeling of blowing snow, Dery and Yau (1998, 1999, 2001) develop and test a
88 parameterization of blowing snow sublimation. Dery and Yau (2002) utilize the model with the
89 ECMWF re-analysis covering 1979 to 1993 and show that most blowing snow sublimation
90 occurs along the coasts and over sea ice with maximums in some coastal areas of 150 mm snow
91 water equivalent (swe) yr^{-1} . Lenearts et al., (2012a) utilized a high resolution regional climate
92 model (RACMO2) to simulate the surface mass balance of the Antarctic ice sheet. They found
93 drifting and blowing snow sublimation to be the most significant ablation term reaching values
94 as high as 200 mm yr^{-1} swe along the coast. Average monthly rates of blowing snow sublimation
95 calculated for Halley Station, Antarctica for the years 1995 and 1996, varied between 0.04
96 (winter) to 0.44 (summer) mm day^{-1} (14.6 and 160 mm yr^{-1} respectively) (King et al. 2001).
97 There has been some recent work done on blowing snow sublimation and transport from field
98 measurements (see for instance Barral et al., 2014 and Trouvilliez et. al., 2014) , but the data are
99 sparse and measurements are only available within the surface layer (< 10 m).

100 While transport of blowing snow is considered to be less important than sublimation in terms
101 of mass balance of the Antarctic ice sheet, erosion and transport of snow by wind can be
102 considerable in certain regions. Das et al., (2013) have shown that blue ice areas are frequently
103 seen in Antarctica. These regions exhibit a negative mass balance as all precipitation that falls is
104 either blown off or sublimated away. Along the coastal regions it has been argued that
105 considerable mass is transported off the coast via blowing snow in preferential areas dictated
106 by topography (Scarchilli et al., 2010). In the Terra Nova Bay region of East Antarctica, manned
107 surface observations show that drifting and blowing snow occurred 80 % of the time in fall and
108 winter and cumulative snow transport was 4 orders about of magnitude higher than snow
109 precipitation. Much of this airborne snow is transported off the continent producing areas of
110 blue ice. Such observations raise questions as to how often and to what magnitude continent to
111 ocean transport occurs. This is important, particularly for Antarctica where the coastline
112 stretches over 17,000 km in length (<https://en.wikipedia.org/wiki/Antarctica>) and where
113 prevailing strong winds through most of the year. Due to the sparsity of observations, the only
114 way to estimate the mass of snow being blown off the coast of Antarctica is by using model

115 parameterizations. Now, for the first time, satellite observations of blowing snow can help
116 better ascertain the magnitude of this elusive quantity.

117 Considering that the accuracy of model data is questionable over Antarctica, and the
118 complicated factors that govern the onset of blowing snow, it is difficult to assess the accuracy
119 of the parameterization of blowing snow sublimation and transport. Recently, methods have
120 been developed to detect the occurrence of blowing snow from direct satellite observations.
121 Palm et al., (2011) show that blowing snow is widespread over much of Antarctica and, in all
122 but the summer months, occurs over 50 % of the time over large areas of East Antarctica. In
123 this paper, we present a technique that uses direct measurements of blowing snow from the
124 CALIPSO satellite lidar combined with The Modern-Era Retrospective analysis for Research and
125 Applications, Version 2 (MERRA-2) re-analysis fields of moisture, temperature and wind to
126 quantify the magnitude of sublimation and mass transport occurring over most of Antarctica
127 (north of 82 south). Section 2 discusses the method used to compute blowing snow sublimation
128 from CALIPSO and MERRA-2 data. In Sect. 3 we show results and compare with previous
129 estimates of sublimation. In Sect. 4 we examine sources of error and their approximate
130 magnitudes. Summary and discussion follow in Sect. 5.

131 **2 Method**

132 The method developed for detection of blowing snow using satellite lidar data (both ICESat and
133 CALIPSO) was presented in Palm et al., (2011). That work showed examples of blowing snow
134 layers as seen by the calibrated, attenuated backscatter data measured by the CALIOP
135 instrument on the CALIPSO satellite. CALIOP (Cloud-Aerosol Lidar with Orthogonal Polarization)
136 is a two wavelength (532 and 1064 nm) backscatter lidar with depolarization at 532 nm and has
137 been operating continuously since June of 2006 (Winker et. al., 2009). In the lower 5 km of the
138 atmosphere, the vertical resolution of the CALIOP backscatter profile is 30 m. The CALIOP
139 backscatter profiles are produced at 20 Hz, which is about a horizontal resolution of 330 m
140 along track. The relatively strong backscattering produced by the earth's surface is used to
141 identify the ground bin in each profile. After the ground signal is detected, each 20 Hz profile is
142 examined for an elevated backscatter signal (above a pre-defined threshold) in the first bin

143 above the ground. If found and the surface wind speed is greater than 4 m s^{-1} , successive bins
144 above that are searched for a 80 % decrease in signal value, which is then the top of the layer.
145 Limited by the vertical resolution of the signal, our approach has the ability to identify blowing
146 snow layers that are roughly 20-30 m or more in thickness. Thus, drifting snow which is
147 confined to 10 m or less and occurs frequently over Antarctica would not be reliably detected.
148 The signal from these layers is likely inseparable from the strong ground return. More
149 information on the blowing snow detection algorithm can be found in Palm et al., (2011).

150 For the work done in this paper we have created a new version of the blowing snow detection
151 algorithm which strives to reduce the occurrence of false positive blowing snow detections. This
152 is done by looking at both the layer average 532 nm depolarization ratio and color ratio
153 (1064/532) and limiting the top height of the layer to 500 m. If a layer is detected, but the top
154 of the layer is above 500 m, it is not included as blowing snow. This height limit helped screen
155 out diamond dust which often stretches for a few kilometers vertically and frequently reaches
156 the ground. It was found that for most blowing snow layers, the depolarization and color ratio
157 averaged about 0.4 and 1.3, respectively (see Fig. 1). If the layer average color or depolarization
158 ratios were out of pre-defined threshold limits, the layer was rejected. The layer average color
159 ratio had to be greater than 1.0 and the depolarization ratio greater than 0.25. The large color
160 ratio is consistent with model simulations for spherical ice particles (Bi et al., 2009). Further,
161 logic was included to reduce misidentification of low cloud as blowing snow by limiting both the
162 magnitude and height of the maximum backscatter signal in the layer. If the maximum signal
163 were greater than $2.0 \times 10^{-1} \text{ km}^{-1} \text{ sr}^{-1}$, the layer was assumed cloud and not blowing snow. In
164 addition, if the maximum backscatter, regardless of its value, occurs above 300 m, the layer is
165 rejected. These changes to the blowing snow detection algorithm slightly decreased (few
166 percent) the overall frequency of blowing snow detections, but we believe we have reduced the
167 occurrence of false positives and the resulting retrievals are now more accurate.

168 Typically, the blowing snow layers are 100–200 m thick, but can range from the minimum
169 detectable height (20 - 30 m) to over 400 m in depth (Mahesh et al., 2003). Often they are seen
170 to be associated with blowing snow storms that cover vast areas of Antarctica and can persist

171 for days. Blowing snow can occur as frequently as 50 % of the time over large regions of East
172 Antarctica in all months but December–February and as frequently as 75 % April through
173 October (Palm et al., 2011). An example of a typical blowing snow layer as seen from the
174 CALIOP backscatter data is shown in Fig. 1.

175 **2.1 MERRA-2 Reanalysis Data**

176 In order to compute blowing snow sublimation, the temperature and relative humidity of the
177 layer must be known. Here we use the MERRA-2 reanalysis (Gelaro, 2017). MERRA-2 is
178 produced with version 5.12.4 of the GEOS atmospheric data assimilation system and contains
179 72 vertical levels from the surface to 0.01 hPa on an approximately $0.5^\circ \times 0.625^\circ$ global grid. The
180 re-analyses are available every 3 hours. To obtain the temperature and relative humidity at a
181 given location, height and time, we use the data from the MERRA-2 grid box which is closest in
182 space and time to the observation. Then we linearly interpolate the temperature, moisture and
183 wind to the height of the CALIPSO observation.

184 We understand that MERRA-2 does not include the effects of blowing snow sublimation on
185 atmospheric moisture and thus may have a dry (and possibly warm) bias. MERRA-2
186 temperature and moisture has not been evaluated over Antarctica but in this section we
187 present a comparison of MERRA-2 temperature and moisture at 2 m height with a surface
188 station and two AWS sites. In Fig. 2 are data from two AWS sites (chosen at random) comparing
189 MERRA-2 and AWS 2 m temperature and relative humidity with respect to ice (RH_{ice}). In both
190 cases MERRA-2 is, on average, slightly colder and moister than the observations (about 1 °C and
191 2%, respectively). Figs. 3a and 3b show MERRA-2 data compared to the surface station at
192 Princess Elisabeth for data taken over 2009-2015. Here MERRA-2 is considerably colder and
193 moister (about 4 °C and 6-8%, respectively). Also shown in Figs. 3c, d and e are the annual mean
194 relative humidity at 2 meters above the surface in 2015 estimated by MERRA-2, ERA-Interim,
195 and AMPS-Polar WRF showing that MERRA-2 is considerably moister than ERA-Interim or
196 AMPS. From these comparisons it is likely that MERRA-2 does not exhibit a dry or warm bias
197 and is rather slightly cold and moist.

198 **2.2 Sublimation**

199 Sublimation of snow occurs at the surface but is greatly enhanced when the snow becomes
200 airborne by the action of wind and turbulence. Once snow particles become airborne, their
201 total surface area is exposed to the air. If the relative humidity of the ambient air is less than
202 100 %, then sublimation will occur. The amount of sublimation is dictated by the number of
203 snow particles in suspension and the relative humidity and temperature of the air. Thus, to
204 estimate sublimation of blowing snow, we must be able to derive an estimate of the number
205 density of blowing snow particles and have knowledge of atmospheric temperature and
206 moisture within the blowing snow layer. The only source of the latter, continent wide at least, is
207 from global or regional models or re-analysis fields. The number density of blowing snow
208 particles can be estimated directly from the CALIOP calibrated, attenuated backscatter data if
209 we can estimate the extinction within the blowing snow layer and have a rough idea of the
210 blowing snow particle radius. The extinction can be estimated from the backscatter through an
211 assumed extinction to backscatter ratio (lidar ratio) for the layer. The lidar ratio, though
212 unknown, would theoretically be similar to that of cirrus clouds, which has been extensively
213 studied. Work done by Josset et al., (2012) and Chen et al., (2002) shows that the extinction to
214 backscatter ratio for cirrus clouds typically ranges between 25 and 30 with an average value of
215 29. However, the ice particles that make up blowing snow are more rounded than the ice
216 particles that comprise cirrus clouds and are on average somewhat smaller (Walden et al.,
217 2003). For this paper, we use a value of 25 for the extinction to backscatter ratio.

218 Measurements of blowing snow particle size have been made by a number of investigators
219 [Schmidt, 1982; Mann et al., 2000; Nishimura and Nemoto, 2005; Walden et al. 2003; Lawson et
220 al., 2006; Gordon and Taylor, 2009], but they were generally made within the first few meters
221 of the surface and may not be applicable to blowing snow layers as deep as those studied here.
222 Most observations have shown a height dependence of particle size ranging from 100 to 200
223 μm in the lower tens of centimeters above the surface to 50–60 μm near 10 m height
224 (Nishimura and Nemoto, 2005). A notable exception is the result of Harder et al., (1996) at the
225 South Pole, who measured the size of blowing snow particles during a blizzard by collecting
226 them on a microscope slide. They report nearly spherical particles with an average effective
227 radius of 15 μm , but the height at which the measurements were made is not reported. From

228 surface observations made at the South Pole, Walden et al., (2003) and Lawson et al., (2006)
229 report an average effective radius for blowing snow particles of 19 and 17 μm , respectively.

230 While no field-measured values for particle radii above roughly 10 m height are available,
231 modeling work indicates that they approach an asymptotic value of about 10-20 μm at heights
232 of 200 m or more (Dery and Yau, 1998). It is also reasonable to assume that snow particles that
233 are high up in the layer are smaller since they have spent more time aloft and have had a
234 greater time to sublimate. Based on the available data, we have defined particle radius ($r(z)$,
235 μm) as a linear function of height:

$$236 \quad r(z) = 40 - \frac{z}{20} \quad (1)$$

237 Thus, for the lowest level of CALIPSO retrieved backscatter (taken to be 15 m – the center of
238 the first bin above the surface), $r(15) = 39.25 \mu\text{m}$ and at the highest level (500 m), $r(500) = 15$
239 μm .

240 The blowing snow particle number density $N(z)$ (particles per cubic meter) can be estimated
241 from the extinction. Note that the extinction is the numerator in equation 2:

$$242 \quad N(z) = \frac{(\beta(z) - \beta_m(z)) S}{2\pi r^2(z)} \quad (2)$$

243 Where $\beta(z)$ is the CALIPSO measured attenuated calibrated backscatter at height z (30 m
244 resolution), $\beta_m(z)$ is the molecular backscatter at height z and S is the extinction to backscatter
245 ratio (25). Here $\beta(z)$ represents the atmospheric backscatter profile through the blowing snow
246 layer. Both $\beta_m(z)$ and $\beta(z)$ have units of $\text{m}^{-1} \text{sr}^{-1}$. We found that the values of $N(z)$ obtained
247 from Eq. (2) for the typical blowing snow layer range from about 5.0×10^4 to 1.0×10^6 particles
248 per cubic meter. This is consistent with the blowing snow model results of Dery and Yau (2002)
249 and the field observations of Mann et al., (2000). A plot of the average particle density for the
250 blowing snow layer in Fig. 1 is shown in Fig. 4. Note that the decrease in particle number
251 density below about 75 m is most likely due to attenuation of the lidar signal as it propagates
252 through the layer. We did not attempt to correct for this and the overall effect is an under

253 estimation of the particle density in this region (which would lead to lower calculated blowing
 254 snow sublimation).

255 Once an estimate of blowing snow particle number density and radii are obtained, the
 256 sublimation rate of the particles can be computed based on the theoretical knowledge of the
 257 process. Following Dery and Yau, (2002), the blowing snow mixing ratio q_b (kg ice / kg air) is
 258 given by:

$$259 \quad q_b(z) = \frac{4\pi \rho_{ice} r^3(z) N(z)}{3 \rho_{air}} \quad (3)$$

260 Or substituting for $N(z)$ (Eq. 2):

$$261 \quad q_b(z) = \frac{2 \rho_{ice} r(z) [\beta(z) - \beta_m(z)] S}{3 \rho_{air}} \quad (4)$$

262 Where ρ_{ice} is the density of ice (917 kg m⁻³), and ρ_{air} the density of air. Again following Dery and
 263 Yau (2002) and others, the sublimation S_b at height z is computed from:

$$264 \quad S_b(z) = \frac{q_b(z) Nu [q_v(z)/q_{is}(z) - 1]}{2 \rho_{ice} r^2(z) [F_k(z) + F_d(z)]} \quad (5)$$

265 Or, letting $\alpha(z)$ be the extinction and substituting for $q_b(z)$:

$$266 \quad S_b(z) = \frac{\alpha(z) Nu [q_v(z)/q_{is}(z) - 1]}{3 \rho_{ice} r(z) [F_k(z) + F_d(z)]} \quad (6)$$

267 Where Nu is the Nusslet number defined as: $Nu = 1.79 + 0.606 Re^{0.5}$

268 with the Reynolds number being: $Re = 2r(z) v_b/v$

269 where v_b is the snow particle fall speed (assumed here to be 0.1 ms⁻¹) and v the kinematic
 270 viscosity of air (1.512x10⁻⁵ m²s⁻¹). q_v is the water vapor mixing ratio of the air (obtained from
 271 model data), q_{is} is the saturation mixing ratio with respect to ice, and F_k and F_d are the heat
 272 conduction and diffusion terms (m s kg⁻¹):

273
$$F_k = \left(\frac{L_s}{R_v T} - 1 \right) \frac{L_s}{K T} \quad (7)$$

274

275
$$F_d = \frac{R_v T}{D e_i(T)} \quad (8)$$

276 Where L_s is the latent heat of sublimation (2.839×10^6 J/Kg), R_v is the individual gas constant for
 277 water vapor (461.5 J kg^{-1} K^{-1}), T is temperature (K), K is the thermal conductivity of air, and D the
 278 coefficient of diffusion of water vapor in air (both D and K are functions of temperature (see
 279 Rogers and Yau, 1989). S_b has units of $\text{kg kg}^{-1} \text{s}^{-1}$. This can be interpreted as the mass of snow
 280 sublimated per mass of air per second.

281 Then the column integrated blowing snow sublimation is:

282
$$Q_s = \rho_{air} \int_{z=0}^{z_{top}} S_b(z) dz \quad (9)$$

283 Where z_{top} is the top of the blowing snow layer and dz is 30 meters. Q_s has units of $\text{kg m}^{-2} \text{s}^{-1}$.
 284 Conversion to mm snow water equivalent (swe) per day is performed by multiplying by a
 285 conversion factor:

286
$$\rho' = 10^3 N_s / \rho_{ice} (1) \quad (10)$$

287 Where N_s is the number of seconds in a day (86,400). The total sublimation amount in mm swe
 288 per day is then:

289
$$Q' = \rho' Q_s \quad (11)$$

290 This computation is performed for every blowing snow detection along the CALIPSO track over
 291 Antarctica. A 1×1 degree grid is then established over the Antarctic continent and each
 292 sublimation calculation (Q') is added to its corresponding grid box over the length of time being
 293 considered (i.e. a year or month). This value is then normalized by the total number of CALIPSO
 294 observations that occurred for that grid box over the time span. The total number of
 295 observations includes all CALIPSO shots within the grid box for which a ground return was

296 detected, regardless of whether blowing snow was detected for that shot or not. Thus, the
297 normalization factor is the total number of shots with ground return detected for that box and
298 is always greater than the number of blowing snow detections (which equals the number of
299 sublimation retrievals). In order for the blowing snow detection algorithm to function, it must
300 first detect the position of the ground return in the backscatter profile. If it cannot do so, it is
301 not considered an observation. Over the interior of Antarctica, failure to detect the surface
302 does not occur often as cloudiness is less than 10 % and most clouds are optically thin. Near the
303 coasts, optically thick clouds become more prevalent. This approach will result in higher
304 sublimation values for those grid boxes that contain a lot of blowing snow detections and vice
305 versa (as opposed to just taking the average of the sublimation values for a grid box).

306 **2.3 Transport**

307 The transport of blowing snow is computed using the CALIPSO retrievals of blowing snow
308 mixing ratio and the MERRA-2 winds. A transport value is computed at each 30 m bin level and
309 integrated through the depth of the blowing snow layer:

$$310 \quad Q_t = \rho_{air} \int_{z=0}^{z_{top}} q_b(z) u(z) dz \quad (12)$$

311 Where $q_b(z)$ is the blowing snow mixing ratio from Eq. (3) and $u(z)$ is the MERRA-2 wind speed
312 at height z and Q_t has units of $\text{kg m}^{-1} \text{s}^{-1}$. The wind speed is linearly interpolated from the
313 nearest two model levels. As with the sublimation, these values are gridded and normalized by
314 the total number of observations. The transport values are computed for each month of the
315 year by summing daily values and then multiplying by the number of seconds in the month
316 (resulting units of kg m^{-1}). The monthly values are then summed to obtain a yearly amount. A
317 further conversion is performed to produce units of $\text{Gt m}^{-1} \text{yr}^{-1}$ by dividing by 10^{12} (1000 kg per
318 metric ton and 10^9 tons per Gt).

319 **3 Results**

320 **3.1 Sublimation**

321 Fig. 5 shows the average blowing snow frequency and corresponding total annual blowing snow
322 sublimation over Antarctica for the period 2007–2015. The highest values of sublimation are
323 along and slightly inland of the coast. Notice that this is not necessarily where the highest
324 blowing snow frequencies are located. Sublimation is highly dependent on the air temperature
325 and relative humidity. For a given value of the blowing snow mixing ratio (q_b), the warmer and
326 drier the air, the greater the sublimation. In Antarctica, it is considerably warmer along the
327 coast but one would not necessarily conclude that it is drier there. However, other authors
328 have noted that the katabatic winds, flowing essentially downslope, will warm and dry the air
329 as they descend (Gallee, 1998, and others). We have examined the MERRA-2 relative humidity
330 (with respect to ice) and indeed, according to the model, it is usually drier along the coast. The
331 model data often shows 90 to 100 % (or even higher) relative humidity for interior portions of
332 Antarctica, while along the coast it is often 70 % or less. It should be noted, however, that this
333 model prediction has never been validated through observations. The combination of warmer
334 and drier air makes a big difference in the sublimation as shown in Fig. 6. For a given relative
335 humidity the sublimation can increase by almost a factor of 100 as temperature increases from
336 -50 to -10 °C. For temperatures greater than -20 °C, sublimation is very dependent on relative
337 humidity, but this dependence lessens somewhat at colder temperatures. Continental interior
338 areas with very high blowing snow frequency that approach 75 % (like the Mega Dune region in
339 East Antarctica) exhibit fairly low values of sublimation because it is very cold and the model
340 relative humidity is high.

341 Fig. 7 shows the annual total sublimation for years 2007–2015. It is evident that the sublimation
342 pattern or magnitude does not change much from year to year. The overall spatial pattern of
343 sublimation is similar to the model prediction of Dery and Yau, (2002) with our results showing
344 noticeably greater amounts in the Antarctic interior and generally larger values near the coast.
345 As previously noted, most sublimation occurs near the coast due mainly to the warmer
346 temperatures. The areas of sublimation maximums near the coast are consistently in the same
347 location year to year, indicating that these areas may experience more blowing snow episodes
348 and possibly more precipitation (availability of snow to become airborne). It is interesting to
349 compare the sublimation pattern with current estimates of Antarctic precipitation. Precipitation

350 is notoriously difficult to quantify over Antarctica due to the scarcity of observations and strong
351 winds producing drifting and blowing snow which can be misidentified as precipitation.
352 Precipitation is often measured by looking at ice cores or is estimated by models. But perhaps
353 the most complete (non-model) measure of Antarctic precipitation come from the CloudSat
354 mission. Palerme et al., (2014) used CloudSat data to construct a map of Antarctic precipitation
355 over the entire continent (north of 82 S). They showed that along the East Antarctic coast and
356 slightly inland, precipitation ranges from 500 to 700 mm swe yr⁻¹ and decreases rapidly inland
357 to less than 50 mm yr⁻¹ in most areas south of 75 S. Their precipitation pattern is in general
358 agreement with the spatial pattern of our sublimation results and the magnitude of our
359 sublimation estimates is in general less than the precipitation amount, with a few exceptions.
360 These occur mostly inland in regions of high blowing snow frequency such as the Megadune
361 region and in the general area of the Lambert glacier. In these regions, our sublimation
362 estimates exceed the CloudSat yearly precipitation estimates. When this occurs, it is likely that
363 either the precipitation estimate is low or the sublimation estimate is too high. Otherwise it
364 would indicate a net negative mass balance for the area unless transport of snow into the
365 region accounted for the difference.

366 Table 1 shows the average sublimation over all grid cells in snow water equivalent and the
367 integrated sublimation amount over the Antarctic continent (north of 82S) for the CALIPSO
368 period in Gt yr⁻¹. Note that the 2006 data include only months June–December (CALIOP began
369 operating in June, 2006) and the 2016 data are only up through October, and do not include the
370 month of February (CALIOP was not operating). To obtain the integrated amount, we take the
371 year average swe (column 1) multiplied by the surface area of Antarctica north of 82S and the
372 density of ice. The average integrated value for the 9 year period 2007–2015 of 393 Gt yr⁻¹ is
373 significantly greater than (about twice) values in the literature obtained from model
374 parameterizations (Lenaerts 2012b). Note also that this amount does not include the area
375 poleward of 82S, the southern limit of CALIPSO observations. If included, and the average
376 sublimation rate over this area were just 4 mm swe per year, this would increase the
377 sublimation total by 10 Gt yr⁻¹. Palerme et al., (2014) has shown that the mean snowfall rate
378 over Antarctica (north of 82 S) from August 2006 to April 2011 is 171 mm yr⁻¹. The average

379 yearly snow water equivalent sublimation from Table I is the average sublimation over the
380 continent (and grounded ice shelves) north of 82 S. For the same time period, our computed
381 CALIPSO-based average blowing snow sublimation is about 50 mm yr⁻¹. This means that on
382 average, over one third of the snow that falls over Antarctica is lost to sublimation through the
383 blowing snow process. In comparison surface sublimation (sublimation of snow on the surface)
384 is considered to be relatively small (about a tenth of airborne sublimation) except in summer
385 (Lenearts 2012a, 2012b).

386 **3.2 Transport**

387 Transport of snow via the wind is generally important locally and does not constitute a large
388 part of the ice sheet mass balance in Antarctica. There are areas where the wind scours away all
389 snow that falls producing a net negative mass balance (i.e. blue ice areas), but in general, the
390 snow is simply moved from place to place over most of the continent. At the coastline,
391 however, this is not the case. There, persistent southerly winds can carry airborne snow off the
392 continent. This can be seen very plainly in Fig. 8 which is a MODIS false color (RGB = 2.1, 2.1, .85
393 μm) image of a large area of blowing snow covering an area about the size of Texas (16,662
394 km²) in East Antarctica. We have found this false color technique to be the best way to visualize
395 blowing snow from passive sensors. The one drawback is that sunlight is required. In Fig. 8,
396 blowing snow shows up as a dirty white, the ice/snow surface (in clear areas) is blue and clouds
397 are generally a brighter white. Also shown in Fig. 8 are two CALIPSO tracks (yellow lines) and
398 their associated retrieved blowing snow backscatter (upper and lower images of CALIOP
399 backscatter). Note that the yellow track lines are drawn only where blowing snow was detected
400 by CALIOP and that not all the CALIOP blowing snow detections are shown. The green dots
401 denote the coastline. Plainly seen along the coast near longitude 145–150E is blowing snow
402 being carried off the continent. In this case, topography might have played a role to funnel the
403 wind in those specific areas. Fig. 9 shows a zoomed in image of this area with the red lines
404 indicating the approximate position of the coastline. Also note that, as evidenced by the times
405 of the MODIS images, this transport began on or before October 13 at 23:00 UTC and continued
406 for at least 7 hours. This region is very close to the area of maximum sublimation seen in Fig. 5

407 and shown to be quite stable from year to year in Fig. 7. Undoubtedly, this continent to ocean
408 transport also occurs in other coastal areas of Antarctica and most often during the dark winter
409 (when MODIS could not see it).

410 In an attempt to better understand the magnitude of this phenomena, we have computed the
411 amount of snow mass being blown off the continent by computing the transport at 342 points
412 evenly spaced (about 60 km apart) along the Antarctic coast using only the v component of the
413 wind. If the v component is positive, then the wind is from south to north. The transport (Eq.
414 (12) using only the v wind component) is computed at each coastal location and then summed
415 over time at that location. The resulting transport is then summed over each coastal location to
416 arrive at a continent-wide value of transport from continent to ocean. Of course this assumes
417 that the coastline is oriented east-west everywhere. This is true of a large portion of Antarctica
418 but there are regional exceptions. Thus we view the results shown in Table II to be an upper
419 limit of the actual continent to ocean transport. Evident from Table II is that most of the
420 transport for East Antarctica occurs in a relatively narrow corridor, with on average over half
421 (51 %) of the transport occurring between 135E and 160E. This is obviously due to the very
422 strong and persistent southerly winds (see Fig. S1) and high blowing snow frequency in this
423 region and is consistent with the conclusions of Scarchilli et al., (2010). In West Antarctica, an
424 even greater fraction (60 %) of the transport off the coast occurs between 80W and 120W.

425 In Fig. 10 we show the magnitude of blowing snow transport for the 2007–2015 timeframe in
426 $\text{Mt km}^{-1} \text{ yr}^{-1}$ as computed from Eq. (12). The magnitude of snow transport, as expected, closely
427 resembles the overall blowing snow frequency pattern as shown in Fig. 5. The maximum values
428 (white areas in Fig. 10) exceed about 3×10^6 tons of snow per km per year. In the supplemental
429 Figs. S1 and S2 we display the MERRA-2 average 10 m wind speed and direction for the years
430 2007–2015. By inspection of Figs. S1 and S2 it is seen that the overall transport in East
431 Antarctica is generally from south to north and obviously dominated by the katabatic wind
432 regime. It is immediately apparent that the average wind speed and direction does not change
433 much from year to year, with the former helping to explain why the average continent-wide
434 blowing snow frequency is also nearly constant from year to year (not shown).

435 **4. Error Analysis**

436 There are a number of factors that can affect the accuracy of the results presented in this work.

437 These include:

438 1) Error in the calibrated backscatter and conversion to extinction

439 2) Errors in the assumed size of blowing snow particles

440 3) Not correcting for possible attenuation above and within the blowing snow layer

441 4) Misidentification of some layers as blowing snow when in fact they were not (false positives)

442 5) Failure to detect some layers (false negatives)

443 6) Errors in the MERRA-2 temperature and moisture data

444 7) Limited spatial sampling

445 The magnitude of some of these can be estimated, others are hard to quantify. For instance, 1),
446 2) and 6) are directly involved in the calculation of sublimation (Eq. 6). The error in extinction,
447 particle radius, temperature and moisture can be estimated. The error associated with the
448 attenuation of the lidar signal above the blowing snow layer (3) is probably very small over the
449 interior of Antarctica, but could be appreciable nearer the coastline. In the interior, clouds are a
450 rare occurrence and when present are usually optically thin. Cloudiness increases dramatically
451 near the coast both in terms of frequency and optical depth. Here the effect of overlying
452 attenuating layers could be appreciable in that it would reduce the backscatter of the blowing
453 snow layer and the derived extinction. This in turn would lead to a lower blowing snow mixing
454 ratio and thus lower sublimation and transport. The effect of attenuation within the layer is
455 unaccounted for here and will also reduce the amount of calculated blowing snow sublimation.

456 With regard to 5) above, the method presented here cannot reliably detect blowing snow layers
457 less than 30 m thick. Therefore, sublimation associated with these layers is not accounted for.
458 Other studies have shown that drifting snow sublimation within the salutation layer can be very
459 significant (Huang et al., 2016). There is a further point to be made with respect to clouds that
460 relates to 5) above. The method we use to detect blowing snow will not work in the presence of
461 overlying, fully attenuating clouds. It is reasonable to suspect that cyclonic storms which

462 impinge upon the Antarctic coast and travel some distance inland would be associated with
463 optically thick clouds and contain both precipitating and blowing snow. Our method would not
464 be able to detect blowing snow during these storms, but we would not count such cases as
465 “observations”, since the ground would not be detected. The point is, blowing snow probably
466 occurs often in wintertime cyclones, but we are not able to detect it. This could lead to an
467 under prediction of blowing snow occurrence, especially near the coast. Also, blowing snow
468 layers less than 20 - 30 m thick would also likely be missed. It is not clear how often these layers
469 occur, but they are known to exist and missing them will produce an underestimate of blowing
470 snow sublimation and transport amounts. With regard to spatial sampling (7 above), unlike
471 most passive sensors, CALIPSO obtains only point measurements along the spacecraft track at
472 or near nadir. On a given day, sampling is poor. CALIPSO can potentially miss a large portion of
473 blowing snow storms such as is evidenced from inspection of Fig. 8. We have seen many
474 examples of such storms in both the MODIS and CALIPSO record. Quantifying the effect of poor
475 sampling on sublimation estimates would be difficult but should be pursued in future work.

476 **4.1 Sensitivity Analysis**

477 A major limitation of this work is the uncertainty inherent in the meteorological data used for
478 obtaining the temperature and moisture within the blowing snow layer. Re-analyses like
479 MERRA-2 do not have the vertical or horizontal resolution to enable an accurate description of
480 the temperature and moisture profile through the blowing snow layer. Also, as mentioned in
481 section 2.1, MERRA-2, or more accurately the GEOS-5 model on which it is based, does not
482 incorporate the effects of blowing snow sublimation on the moisture within the layer. Even so,
483 we have already shown that MERRA-2 is moist compared to surface observations and to other
484 models. Thus we do not feel that using the MERRA-2 moisture will cause a large overestimation
485 of blowing snow sublimation. However, it is important to examine the effects of moisture on
486 the calculated sublimation. To demonstrate this we have taken one CALIPSO track with blowing
487 snow (shown in Fig. 11a) and plotted the MERRA-2 humidity (wrt ice) and the calculated
488 blowing snow sublimation along the track. We then increased the moisture amount by 5 and
489 10% to see the effect on the calculated sublimation. The temperature was not changed. In Figs.

490 11b – 11d the MERRA-2 relative humidity is the dark solid line, MERRA-2 temperature is the
491 dotted line and the calculated blowing snow sublimation is the thin black line. The temperature
492 and moisture shown are the MERRA-2 averages through the blowing snow layer. Figure 11b
493 shows the unperturbed MERRA-2 moisture and the resulting blowing snow sublimation
494 (integrated through the layer). In Fig 11c and 11d we have increased the MERRA-2 relative
495 humidity by 5 and 10%, respectively. The effect on the average blowing snow sublimation is
496 marked. A 10% increase in relative humidity produces about a 30% reduction in the calculated
497 blowing snow sublimation. This exercise demonstrates the non-linear effect of the moisture
498 level on the calculated sublimation.

499 If we assume then that the error in moisture is 10%, we must accept that the resulting blowing
500 snow sublimation could be 30% too high. But is that realistic, given the fact that the MERRA-2
501 data were shown to be moist compared to observation and other models? We do not think so.
502 Rather we take the error in MERRA-2 moisture to be 5%. This produces an 18% over estimation
503 of sublimation (Fig. 11b compared to Fig. 11c). This error must be combined with other errors
504 such as extinction, particle radius and temperature. Here we assume the extinction error to be
505 20 %, the particle radius error 10 % and the temperature error 5%. In Eq. (6) these terms are
506 multiplicative. The total error in sublimation is then:

$$507 \quad \pm 1 - (0.8 * 0.9 * 0.95) + 0.18 = \pm 0.50$$

508 This indicates that the sublimation values derived in this work should be considered to have an
509 error bar of ± 50 %. The error in computed transport involves error in wind speed and the
510 blowing snow mixing ratio, the latter being dependent on extinction and particle size. If we
511 assume wind speed has an error of 20 %, extinction 20 % and particle size 10 %, the total error
512 in transport is:

$$513 \quad \pm 1 - (0.8 * 0.8 * 0.9) = \pm 0.42$$

514 **5. Summary and Discussion**

515 This paper presents the first estimates of blowing snow sublimation and transport over
516 Antarctica that are based on actual observations of blowing snow layers from the CALIOP space
517 borne lidar onboard the CALIPSO satellite. We have used the CALIOP blowing snow retrievals
518 combined with MERRA-2 model re-analyses of temperature and moisture to compute the
519 temporal and spatial distribution of blowing snow sublimation and transport over Antarctica for
520 the first time. The results show that the maximum sublimation, with annual values exceeding
521 250 (± 125) mm swe, occurs within roughly 200 km of the coast even though the maximum
522 frequency of blowing snow most often occurs considerably further inland. This is a result of the
523 warmer and drier air near the coast which substantially increases the sublimation. In the
524 interior, extremely cold temperatures and high model relative humidity lead to greatly reduced
525 sublimation. However, the values obtained in parts of the interior (notably the Megadune
526 region of East Antarctica - roughly 75 to 82S and 120 to 160E) are considerably higher than
527 prior model estimates of Dery and Yau (2002) or Lenaerts et al., 2012a). This is most likely due
528 to the very high frequency of occurrence of blowing snow as detected from CALIOP data in this
529 region which is not necessarily captured in models (Lenaerts et al., 2012b).

530 The spatial pattern of the transport of blowing snow follows closely the pattern of blowing
531 snow frequency. The maximum transport values are about 5 Megatons per km per year and
532 occur in the Megadune region of East Antarctica with other locally high values at various
533 regions near the coast that generally correspond to the maximums in sublimation. We
534 attempted to quantify the amount of snow being blown off the Antarctic continent by
535 computing the transport along the coast using only the v component of the wind. While this
536 may produce an overestimate of the transport (since the Antarctic coast is not oriented east-
537 west everywhere), we find the amount of snow blown off the continent to be significant and
538 fairly constant from year to year. The average off-continent transport for the 9 year period
539 2007–2015 was 3.68 Gt yr^{-1} with about two thirds of that coming from East Antarctica and over
540 one third from a relatively small area between longitudes 135E and 160E.

541 Over the nearly 11 years of data, the inter-annual variability of continent wide sublimation
542 (Table 1) can be fairly large – 10 to 15 % - and likely the result of precipitation variability and or

543 changes in the MERRA-2 temperature and moisture data. There seems to be a weak trend to
544 the sublimation data with earlier years having greater sublimation than more recent years.
545 However, based on the short length of the time series and the likely magnitude of error in the
546 sublimation estimates, the trend cannot be considered statistically significant.

547 The overall spatial pattern of blowing snow sublimation is consistent with previous modelling
548 studies (Dery and Yau, 2002 and Lenaerts et al., 2012a). However, we find the Antarctic
549 continent-wide integrated blowing snow sublimation to be larger than previous studies such as
550 Lenaerts et al., (2012a) (393 ± 196 vs roughly 190 Gt yr^{-1}), even though the observations include
551 only the area north of 82° S . The maximum in sublimation is about $250 (\pm 125)$ mm swe per year
552 near the coast between longitudes 140E and 150E and seems to occur regularly throughout the
553 11 year data record. There are a number of reasons for the higher sublimation values in this
554 study compared to prior estimates. 1) The depth of the layer: the average blowing snow layer
555 depth as determined from the CALIOP measurements is 120 m. Layers as high as 200 - 300 m
556 are not uncommon. It is likely that models such as those cited above do not always capture the
557 full depth of blowing snow layers, thus producing a smaller column-integrated sublimation
558 amount. 2) We only compute sublimation from blowing snow layers that are known to exist
559 (meaning they have been detected from actual backscatter measurements). Models, on the
560 other hand, must infer the presence of blowing snow from pertinent variables within the
561 model. The existence of blowing snow is not easy to predict. It is a complicated function of the
562 properties of the snowpack, surface temperature, relative humidity and wind speed. Snowpack
563 properties include the dendricity, sphericity, grain size and cohesion, all of which can change
564 with the age of the snow. In short, it is very difficult for models to predict exactly when and
565 where blowing snow will occur, much less the depth that blowing snow layers will attain. 3) The
566 lack of blowing snow physics within the MERRA-2 reanalysis. This produces perhaps the largest
567 uncertainty in the derived results. It was shown that MERRA-2 is slightly colder and moister
568 than some surface measurements and moister compared to other re-analyses. However, given
569 the limited number of comparisons, a definitive conclusion on the accuracy of MERRA-2 data
570 cannot be drawn. Since the model on which MERRA-2 re-analysis is based (GEOS-5) does not
571 include blowing snow (and thus blowing snow feed backs on moisture and temperature), it is

572 likely that our estimates of blowing snow sublimation are probably too high. However, the fact
573 that we do not include blowing snow layers less than 30 m in depth and are not able to detect
574 blowing snow beneath thick clouds layers means that we are missing potentially important
575 contributions to sublimation. An addition, the retrieved blowing snow number density below
576 about 80 m is probably too low for layers greater than 120 m in depth because of lidar signal
577 attenuation. This will act to erroneously reduce the calculated sublimation. While we estimate
578 an upper limit on the error of our blowing snow sublimation results as 50%, we believe that the
579 error is considerably less than that.

580 Future work should involve coupling the CALIPSO blowing snow observations with a regional
581 model that contains blowing snow physics. This could increase the accuracy of the calculated
582 blowing snow sublimation by incorporating the moisture feedback processes within the layer
583 that have been neglected here.

584 **Data Availability**

585 The CALIPSO calibrated attenuated backscatter data used in this study can be obtained from
586 the NASA Langley Atmospheric Data Center at: [https://earthdata.nasa.gov/about/daacs/daac-](https://earthdata.nasa.gov/about/daacs/daac-asdc)
587 [asdc](https://earthdata.nasa.gov/about/daacs/daac-asdc)

588 The MERRA-2 data are available from the Goddard Earth Sciences Data and Information
589 Services Center (GESDISC) at: https://disc.gsfc.nasa.gov/datareleases/merra_2_data_release.

590 The blowing snow data (layer backscatter, height, etc.) are available through the corresponding
591 author and will be made publicly available through the NASA Langley Atmospheric Data Center
592 in the near future.

593 **Acknowledgements**

594 This research was performed under NASA contracts NNH14CK40C and NNH14CK39C. The
595 authors would like to thank Dr. Thomas Wagner and Dr. David Considine for their support and
596 encouragement. The CALIPSO data used in this study were the DOI:

597 10.5067/CALIOP/CALIPSO/LID_L1-ValStage1-V3-40_L1B-003.40 data product obtained from the
598 NASA Langley Research Center Atmospheric Science Data Center. We also acknowledge the
599 Global Modeling and Assimilation Office (GMAO) at Goddard Space Flight Center who supplied
600 the MERRA-2 data.

601 **References**

602 Barral, H., C. Genthon, A. Trouvilliez, C. Brun, and C. Amory: Blowing snow in coastal Adélie
603 Land, Antarctica: three atmospheric-moisture issues. *The Cryosphere*, 8, 1905–1919, 2014
604 www.the-cryosphere.net/8/1905/2014/ doi:10.5194/tc-8-1905-2014

605 Bi, L., Yang, P., Kattawar, G. W., Baum, B. A., Hu, Y. X., Winker, D. M., Brock, R. S., and J. Q. Lu, J.
606 Q.: Simulation of the color ratio associated with the backscattering of radiation by ice particles
607 at the wavelengths of 0.532 and 1.064 μm , *J. Geophys. Res.*, 114, D00H08,
608 doi:10.1029/2009JD011759, 2009.

609 Bintanja, R., and Krieken, F.: Magnitude and pattern of Arctic warming governed by the
610 seasonality of radiative forcing, *Sci. Rep-Uk*, 6, doi: 10.1038/srep38287, 2016.

611 Bowling, L. C., Pomeroy, J. W., and Lettenmaier, D. P.: Parameterization of blowing-snow
612 sublimation in a macroscale hydrology model, *J Hydrometeor.*, 5, 745-762, doi: 10.1175/1525-
613 7541(2004)005<0745:Pobsia>2.0.Co;2, 2004.

614 Bromwich, D. H., Nicolas, J. P., Monaghan, A. J., Lazzara, M. A., Keller, L. M., Weidner, G. A., and
615 Wilson, A. B.: Central West Antarctica among the most rapidly warming regions on Earth, *Nat.*
616 *Geosci.*, 6, 139-145, doi: 10.1038/Ngeo1671, 2013.

617 Bromwich, D. H.: Snowfall in high southern latitudes. *Rev Geophys* 26:149–168, 1988

618 Chen, W. N., Chiang, C. W., and Nee, J. B.: Lidar ratio and depolarization ratio for cirrus clouds,
619 *Appl. Optics*, 41, 6470-6476, doi: 10.1364/Ao.41.006470, 2002.

620 Church, J. A., Clark, P. U., Cazenave, A., Gregory, J. M., Jevrejeva, S., Levermann, A., Merrifield,
621 M. A., Milne, G. A., Nerem, R. S., Nunn, P. D., Payne, A. J., Pfeffer, W. T., Stammer, D., and

622 Unnikrishnan, A. S.: Sea level change, in: Climate change 2013: The Physical science basis.
623 Contribution of working group I to fifth assessment report of the Intergovernmental panel of
624 climate change, edited by: Stocker, T. F., Qin, D., Plattner, G. K., Tignor, M., Allen, S. K.,
625 Boschung, J., Nauels, A., Xia, Y., Bex, V., and Midgley, P. M., Cambridge University Press,
626 Cambridge, UK and New York, USA, 2013.

627 Das, I., Bell, R. E., Scambos, T. A., Wolovick, M., Creyts, T. T., Studinger, M., Frearson, N.,
628 Nicolas, J. P., Lenaerts, J. T. M., and van den Broeke, M. R.: Influence of persistent wind scour
629 on the surface mass balance of Antarctica, *Nat. Geosci.*, 6, 367-371, doi: 10.1038/Ngeo1766,
630 2013.

631 Dery, S. J., and Yau, M. K.: Large-scale mass balance effects of blowing snow and surface
632 sublimation, *J. Geophys. Res.-Atmos.*, 107, doi: 10.1029/2001jd001251, 2002.

633 Dery, S. J. and Yau, M. K.: Simulation of Blowing Snow in the Canadian Arctic Using a Double-
634 Moment Model, *Boundary-Layer Meteorology*, 99, 297–316, 2001.

635 Dery, S. J. and M.K. Yau, M. K.: A Bulk Blowing Snowmodel, *Boundary-Layer Meteorology*, 93,
636 237–251, 1999.

637 Dery, S. J., Taylor, P. A., Xiao, J.: The Thermodynamic Effects of Sublimating, Blowing Snow in
638 the Atmospheric Boundary Layer, Dept. of Atmospheric and Oceanic Sciences, McGill
639 University, 805 Sherbrooke St. W., Montréal, Québec, H3A 2K6 Canada, *Boundary-Layer*
640 *Meteorology*, 89, 251–283, 1998.

641 Frezzotti, M., Gandolfi, S., and Urbini, S.: Snow megadunes in Antarctica: Sedimentary structure
642 and genesis, *J. Geophys. Res.-Atmos.*, 107, doi: 10.1029/2001jd000673, 2002.

643 Gallée, H.: A simulation of blowing snow over the Antarctic ice sheet, *Ann Glaciol*, 26, 203–205,
644 1998.

645 Gelaro, R., W. McCarty, M. Suarez, R. Todling, A. Molod, L. Takacs, C. Randles, A. Darmenov, M.
646 Bosilovich, R. Reichle, K. Wargan, L. Coy, R. Cullather, C. Draper, S. Akella, V. Buchard, A. Conaty,
647 A. da Silva, W. Gu, G. Kim, R. Koster, R. Lucchesi, D. Merkova, J. Nielsen, G. Partyka, S. Pawson,
648 W. Putman, M. Rienecker, S. Schubert, M. Sienkiewicz, and B. Zhao, 2017: The Modern-Era
649 Retrospective Analysis for Research and Applications, Version 2 (MERRA-2). *J. Climate*.
650 doi:10.1175/JCLI-D-16-0758.1, in press.

651 Gordon, M., and Taylor, P. A.: Measurements of blowing snow, Part I: Particle shape, size
652 distribution, velocity, and number flux at Churchill, Manitoba, Canada, *Cold Reg. Sci. Technol.*,
653 55, 63-74, doi: 10.1016/j.coldregions.2008.05.001, 2009.

654 Harder, S. L., Warren, S. G., Charlson, R. J., and Covert, D. S.: Filtering of air through snow as a
655 mechanism for aerosol deposition to the Antarctic ice sheet, *J. Geophys. Res.-Atmos.*, 101,
656 18729-18743, doi: 10.1029/96jd01174, 1996.

657 Huang, N., Dai, X., and Zhang, J.: The impacts of moisture transport on drifting snow
658 sublimation in the saltation layer, *Atmos. Chem. Phys.*, 16, 7523-7529, doi:10.5194/acp-16-
659 7523-2016, 2016.

660 Josset, D., Pelon, J., Garnier, A., Hu, Y. X., Vaughan, M., Zhai, P. W., Kuehn, R., and Lucker, P.:
661 Cirrus optical depth and lidar ratio retrieval from combined CALIPSO-CloudSat observations
662 using ocean surface echo, *J. Geophys. Res.-Atmos.*, 117, doi: 10.1029/2011jd016959, 2012.

663 King, J. C., Anderson, P. S., and Mann, G. W.: The seasonal cycle of sublimation at Halley,
664 Antarctica, *J. Glaciol.*, 47, 1-8, doi: 10.3189/172756501781832548, 2001.

665 Lawson, R. P., Baker, B. A., Zmarzly, P., O'Connor, D., Mo, Q. X., Gayet, J. F., and Shcherbakov,
666 V.: Microphysical and optical properties of atmospheric ice crystals at South Pole station, *J.*
667 *Appl. Meteor. Climatol.*, 45, 1505-1524, doi: 10.1175/Jam2421.1, 2006.

668 Lenaerts, J. T. M., van den Broeke, M. R., Dery, S. J., van Meijgaard, E., van de Berg, W. J., Palm,
669 S. P., and Rodrigo, J. S.: Modeling drifting snow in Antarctica with a regional climate model: 1.

670 Methods and model evaluation, *J. Geophys. Res.-Atmos.*, 117, doi: 10.1029/2011jd016145,
671 2012a.

672 Lenaerts, J. T. M., van den Broeke, M. R., van de Berg, W. J., van Meijgaard, E., and Munneke, P.
673 K.: A new, high-resolution surface mass balance map of Antarctica (1979-2010) based on
674 regional atmospheric climate modeling, *Geophys. Res. Lett.*, 39, doi: 10.1029/2011gl050713,
675 2012b.

676 Mahesh, A., Eager, R., Campbell, J. R., and Spinhirne, J. D.: Observations of blowing snow at the
677 South Pole, *J. Geophys. Res.*, 108(D22), 4707, doi:10.1029/2002JD003327, 2003.

678 Mann, G. W., Anderson, P. S., and Mobbs, S. D.: Profile measurements of blowing snow at
679 Halley, Antarctica, *J. Geophys. Res.-Atmos.*, 105, 24491-24508, doi: 10.1029/2000jd900247,
680 2000.

681 Nishimura, K., and Nemoto, M.: Blowing snow at Mizuho station, Antarctica, *Philos. T Roy Soc.*
682 *A*, 363, 1647-1662, doi: 10.1098/rsta.2005.1599, 2005.

683 Palerme, C., Kay, J. E., Genthon, C., L'Ecuyer, T., Wood, N. B., and Claud, C.: How much snow
684 falls on the Antarctic ice sheet?, *Cryosphere*, 8, 1577-1587, doi: 10.5194/tc-8-1577-2014, 2014.

685 Palm, S. P., Yang, Y. K., Spinhirne, J. D., and Marshak, A.: Satellite remote sensing of blowing
686 snow properties over Antarctica, *J. Geophys. Res.-Atmos.*, 116, doi: 10.1029/2011jd015828,
687 2011.

688 Pomeroy, J. W., Gray, D. M., and Landine, P. G.: The Prairie Blowing Snow Model -
689 Characteristics, Validation, Operation, *J. Hydrol.*, 144, 165-192, doi: 10.1016/0022-
690 1694(93)90171-5, 1993.

691 Pomeroy, J. W., Marsh, P., and Gray, D. M.: Application of a distributed blowing snow model to
692 the arctic, *Hydrol. Process*, 11, 1451-1464, 1997.

693 Przybylak, R.: Recent air-temperature changes in the Arctic, *Annals of Glaciology*, Vol 46, 2007,
694 46, 316-324, doi: 10.3189/172756407782871666, 2007.

695 Rogers, R. R., and Yau, M. K.: *A Short Course in Cloud Physics*, 3rd. ed., Pergamon Press, 290 pp.,
696 1989.

697 Scarchilli, C., Frezzotti, M., Grigioni, P., De Silvestri, L., Agnoletto, L., and Dolci, S.: Extraordinary
698 blowing snow transport events in East Antarctica, *Clim. Dynam.*, 34, 1195-1206, doi:
699 10.1007/s00382-009-0601-0, 2010.

700 Schmidt, R. A.: Vertical profiles of wind speed, snow concentration and humidity and blowing
701 snow, *Boundary-layer Meteorol.*, 23, 223-246, 1982.

702 Steig, E. J., Schneider, D. P., Rutherford, S. D., Mann, M. E., Comiso, J. C., and Shindell, D. T.:
703 Warming of the Antarctic ice-sheet surface since the 1957 International Geophysical Year,
704 *Nature*, 457, 459-462, doi: 10.1038/nature07669, 2009.

705 Tabler, R. D., Benson, C. S., Santana, B. W., and Ganguly, P.: Estimating Snow Transport from
706 Wind-Speed Records - Estimates Versus Measurements at Prudhoe Bay, Alaska, *Proceedings of*
707 *the Western Snow Conference : Fifty-Eighth Annual Meeting*, 61-72, 1990.

708 Tabler, R. D.: Estimating the transport and evaporation of blowing snow *Snow Management on*
709 *the Great Plains*, July 1985, Swift Current, Sask, Great Plains Agricultural Council Publication No.
710 73, University of Nebraska, Lincoln, NE, 1975, pp. 85-105.

711 Trouvilliez, A., Naaim, F., Genthon, C., Piard, L., Favier, V., Bellot, H., Agosta, C., Palerme, C.,
712 Amory, C., and Gallée, H.: Blowing snow observation in Antarctica: A review including a new
713 observation system in Adélie Land, *Cold Reg. Sci. Technol.*,
714 doi:10.1016/j.coldregions.2014.09.005, 2014.

715 Van den Broeke, M., Konig-Langlo, G., Picard, G., Munneke, P. K., and Lenaerts, J.: Surface
716 energy balance, melt and sublimation at Neumayer Station, East Antarctica, *Antarct. Sci.*, 22,
717 87-96, doi: 10.1017/S0954102009990538, 2010.

718 Walden, V. P., Warren, S. G., and Tuttle, E.: Atmospheric ice crystals over the Antarctic Plateau
719 in winter, *J. Appl. Meteor. Climatol.*, 42, 1391-1405, doi: 10.1175/1520-
720 0450(2003)042<1391:Aicota>2.0.Co;2, 2003.

721 Winker, D. M., Vaughan, M. A., Omar, A., Hu, Y. X., Powell, K. A., Liu, Z. Y., Hunt, W. H., and
722 Young, S. A.: Overview of the CALIPSO mission and CALIOP data processing algorithms, *J. Atmos.*
723 *Oceanic Technol.*, 26, 2310-2323, doi: 10.1175/2009jtecha1281.1, 2009.

724 Table I. The year average sublimation per year (average off all grid boxes) and the integrated
 725 sublimation over the Antarctic continent (north of 82S). * 2006 and 2016 consist of only 7 and 9
 726 months of observations, respectively.

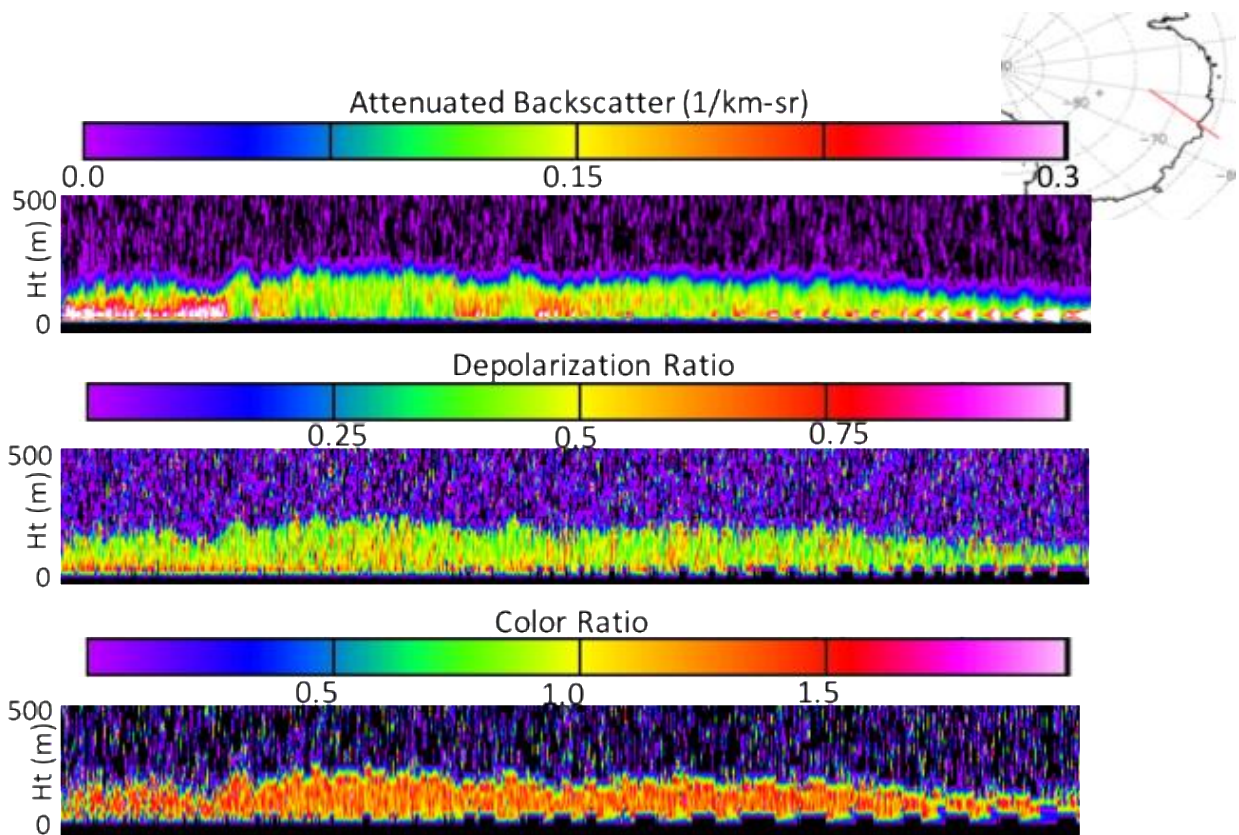
Year	Average Sublimation (mm _{we})	Integrated Sublimation (Gt _{yr} ⁻¹)
2006*	28.3	255
2007	56.8	514
2008	49.2	446
2009	45.3	409
2010	42.9	388
2011	47.6	431
2012	44.4	402
2013	47.7	432
2014	41.5	376
2015	41.3	374
2016*	33.2	301
AVG	43.5*	393.4*

727

728 Table II. The total transport (Gt yr⁻¹) from continent to ocean for various regions in Antarctica
 729 for 2007–2015.

Year	East Antarctica	West Antarctica	135E–160E	80W–120W
2007	2.52	1.29	1.72	0.82
2008	2.20	1.43	1.21	0.90
2009	2.63	1.27	1.51	0.78
2010	2.26	1.15	1.38	0.73
2011	2.04	1.04	1.13	0.64
2012	2.49	1.21	1.41	0.73
2013	2.54	1.41	1.26	0.83
2014	2.55	1.02	1.49	0.67
2015	2.76	1.38	1.58	0.69
Avg	2.44	1.24	1.41	0.75

730

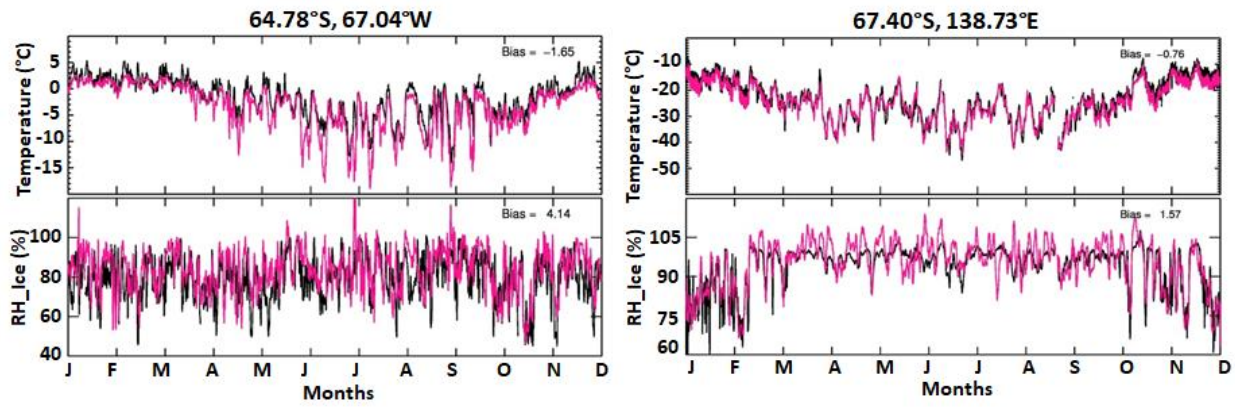


731

732 Figure 1. A typical Antarctic blowing snow layer as measured by CALIPSO on May 28, 2015 at
 733 17:08:41 – 17:11:33 UTC. Displayed (from top to bottom) are the 532 nm calibrated, attenuated
 734 backscatter, the depolarization ratio at 532 nm, and the color ratio (1064 nm / 532 nm).

735

736

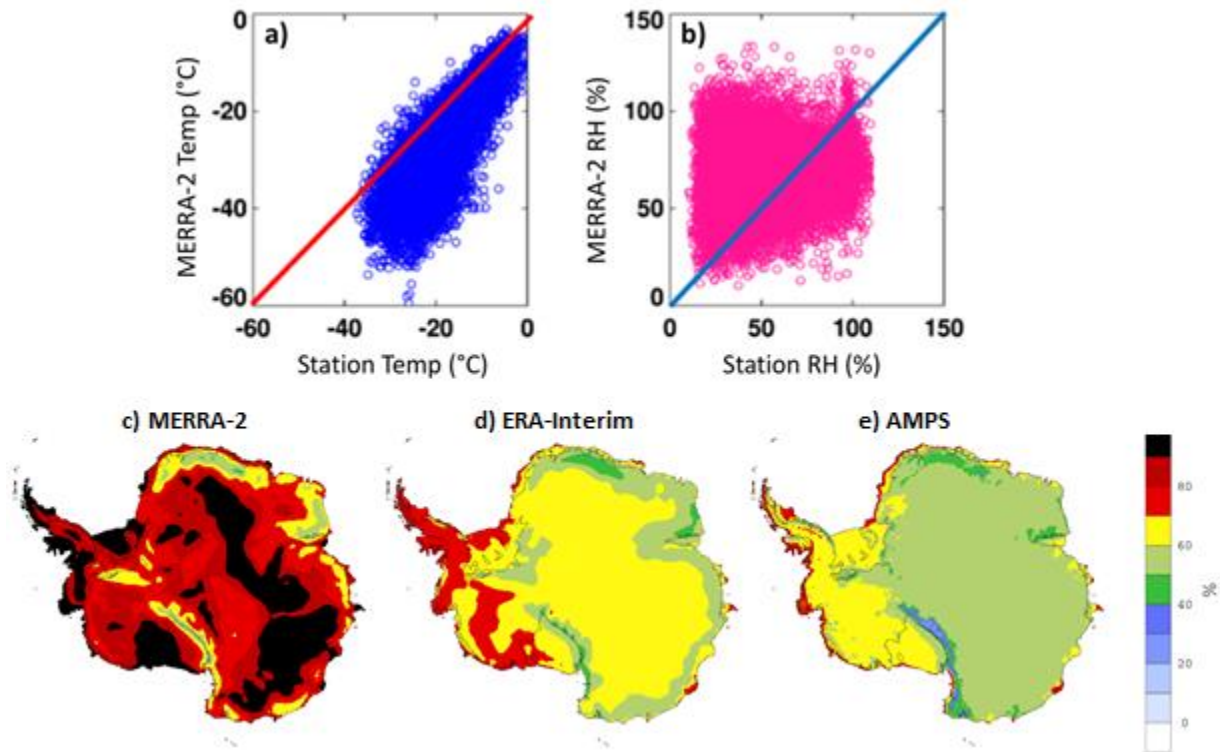


737

738 Figure 2. A comparison of 2 m MERRA-2 temperature and moisture (pink) with measurements from 2
739 AWS stations for 2016.

740

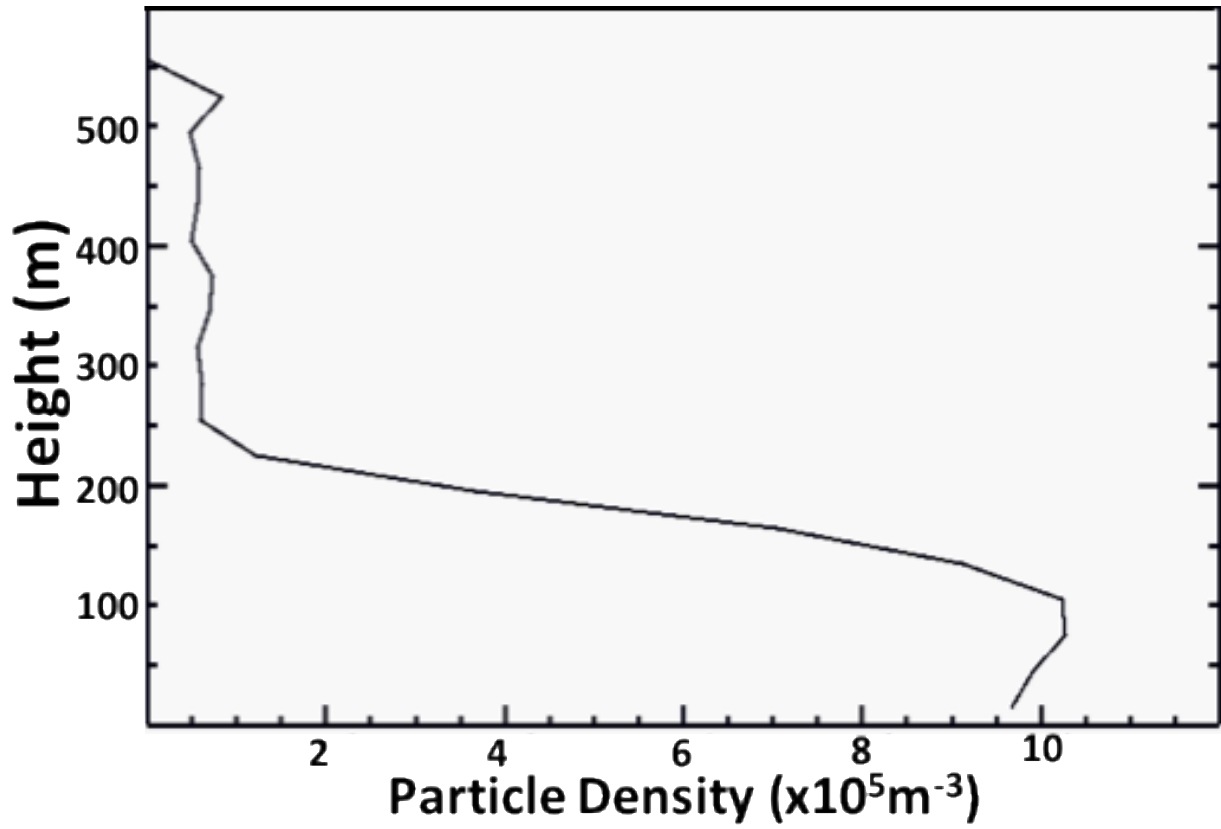
741



742

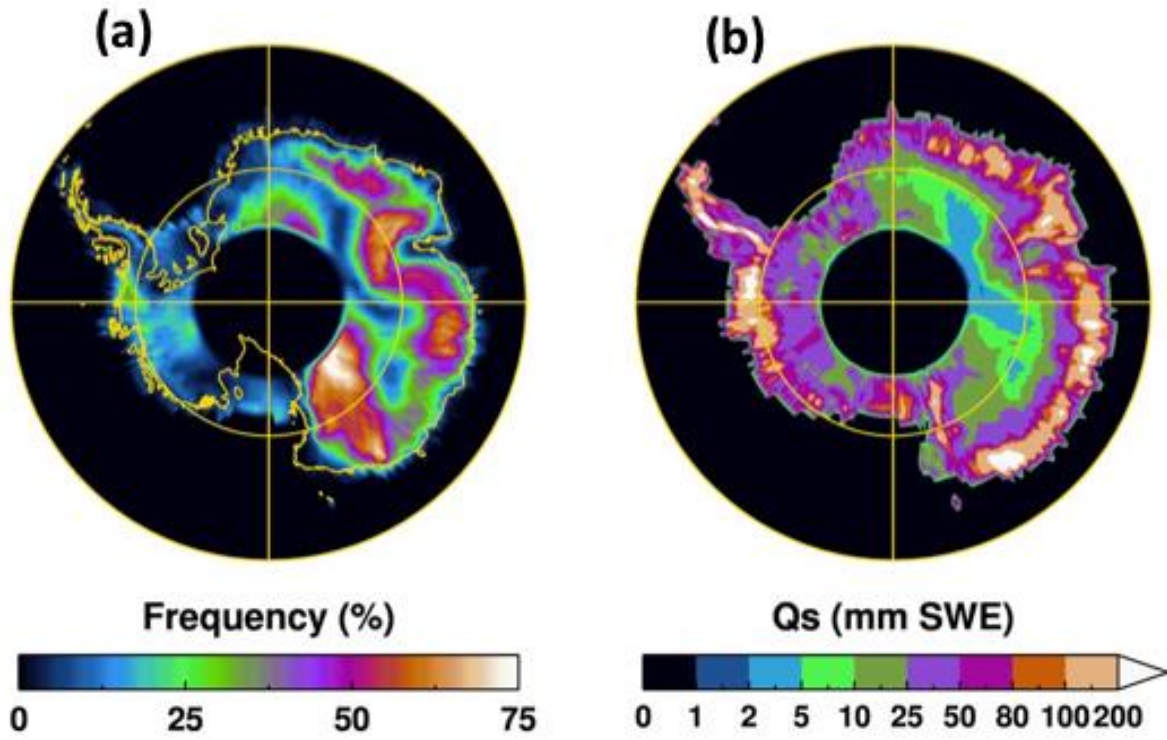
743 Figure 3. (a) A comparison of MERRA-2 2 m temperature and (b) relative humidity with respect
744 to ice for the period 2009-2015 at Princess Elisabeth Station, Antarctica. (c-e) Annual mean
745 relative humidity at 2 meters above the surface in 2015 estimated by (c) MERRA-2, (d) ERA-
746 Interim, and (e) AMPS-Polar WRF.

747



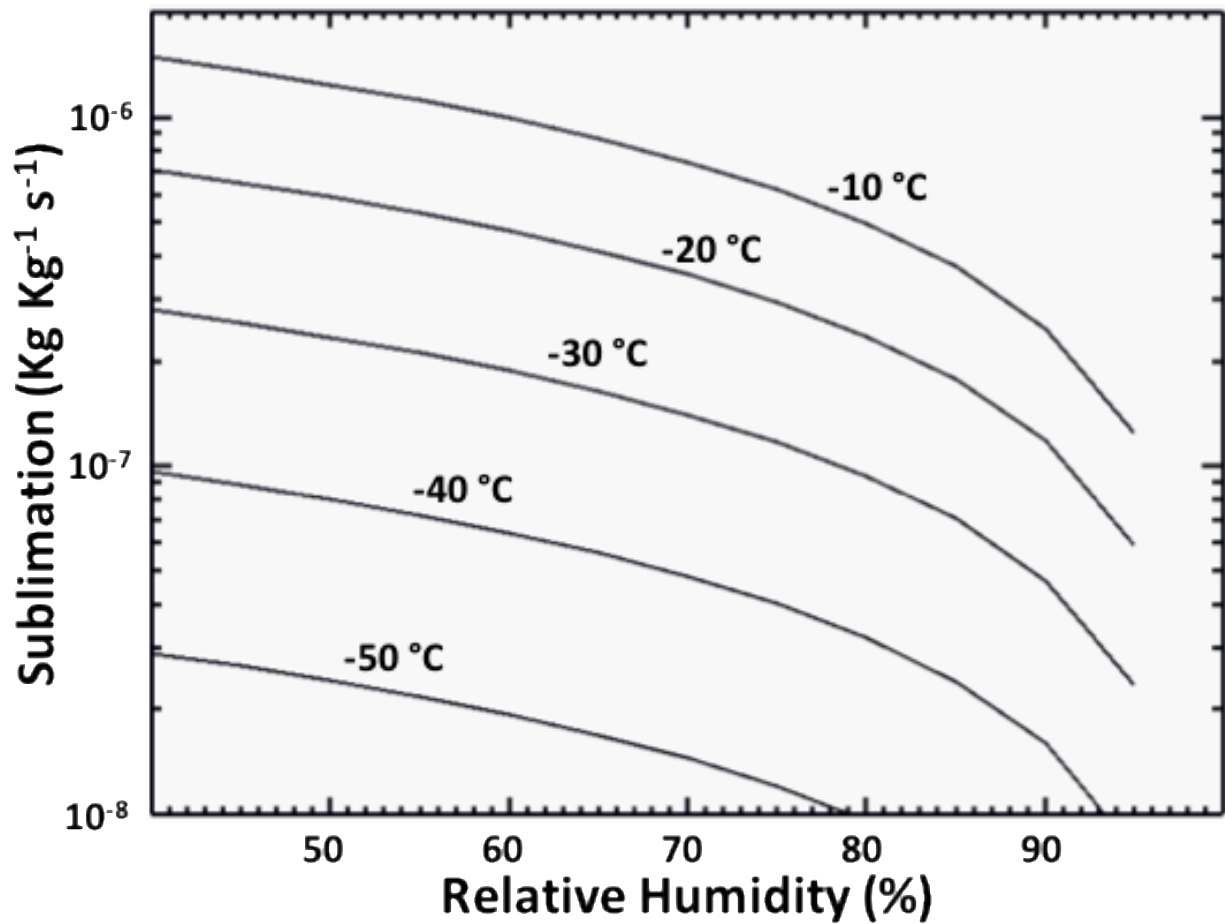
748

749 Figure 4. Average particle density profile (Eq. 2) through the blowing snow layer shown in Fig. 1.



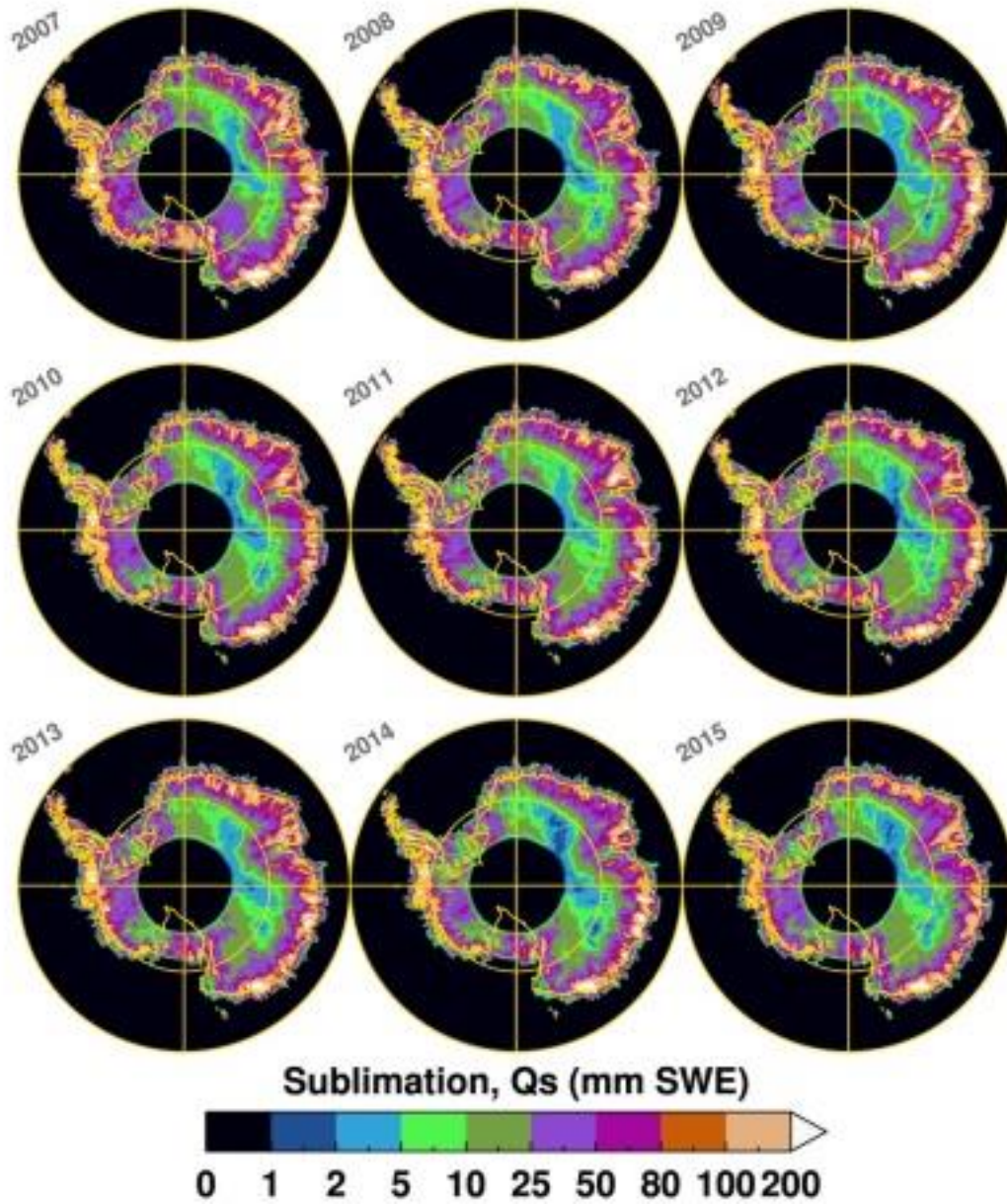
750

751 Figure 5. (a) The average April through October blowing snow frequency for the period 2007–
 752 2015. (b) The average annual blowing snow sublimation for the same period as in (a).



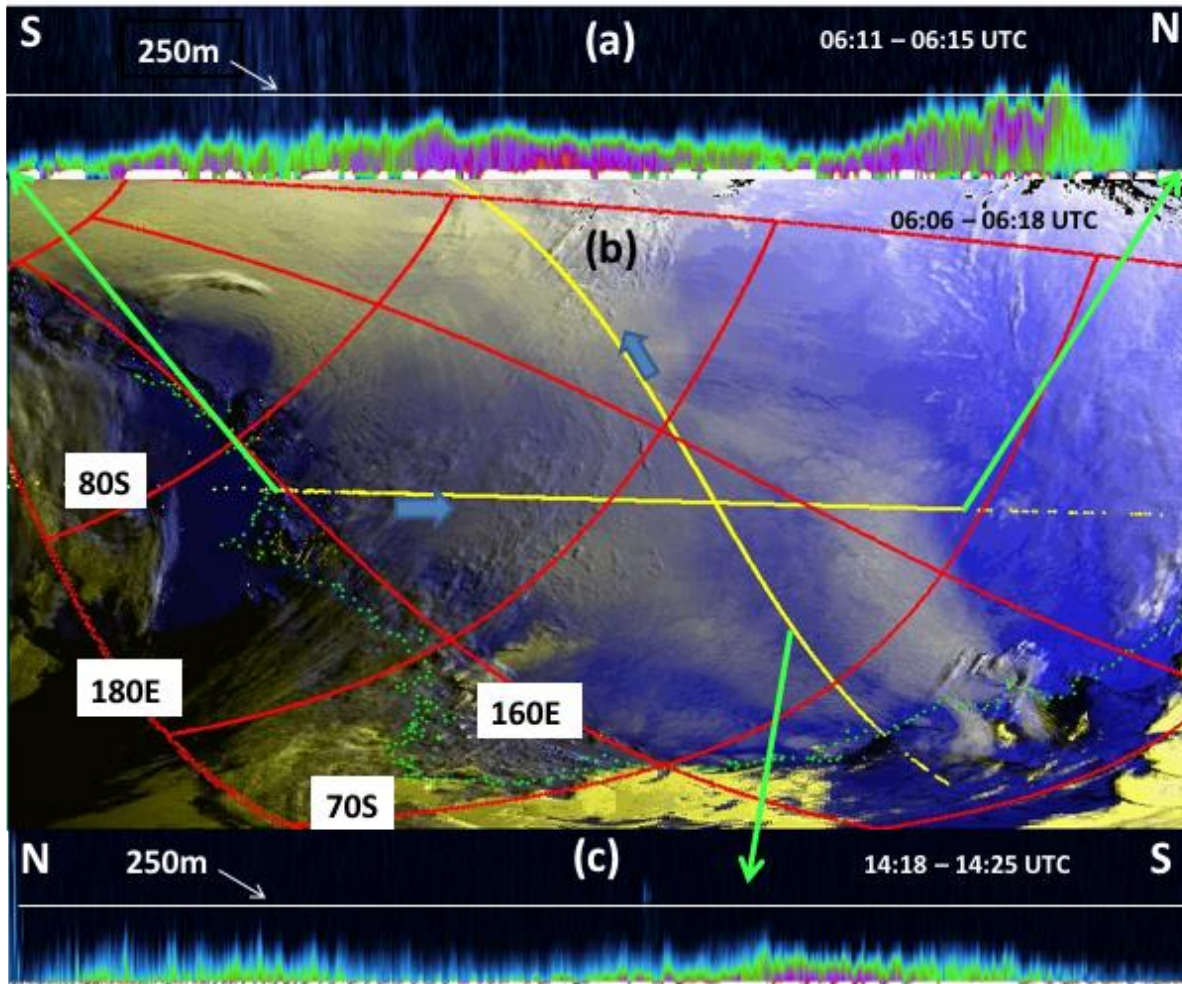
753

754 Figure 6. Computed blowing snow sublimation rate using Eqs. (3) and (4) as function of relative
 755 humidity for varying air temperatures. The particle density value used in Eq. (3) was 10^6 m^{-3}
 756 which corresponds to a blowing snow mixing ratio (q_b) of $4.7 \times 10^{-5} \text{ kg kg}^{-1}$



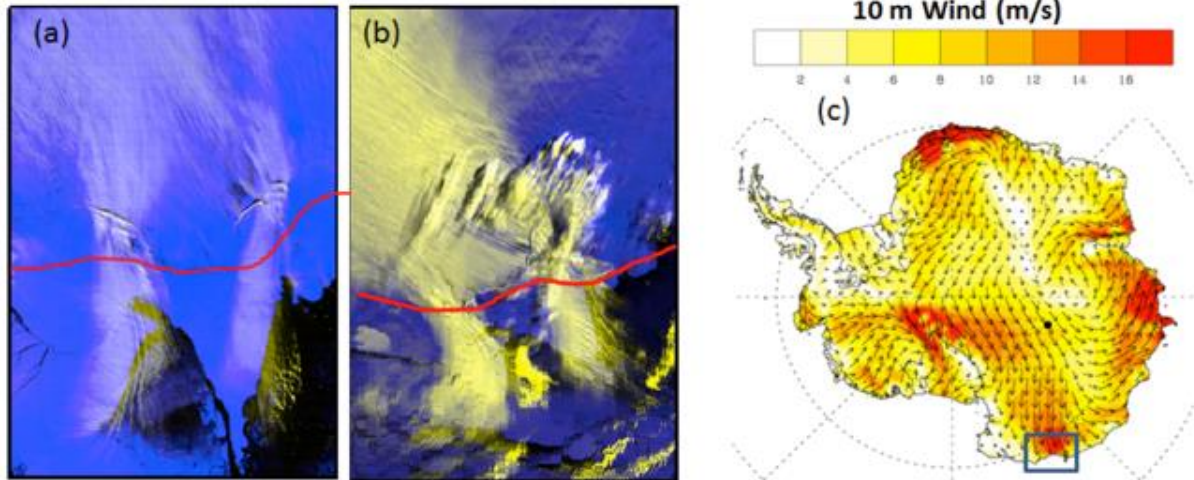
757

758 Figure 7. Blowing snow total sublimation over Antarctica by year for 2007–2015.



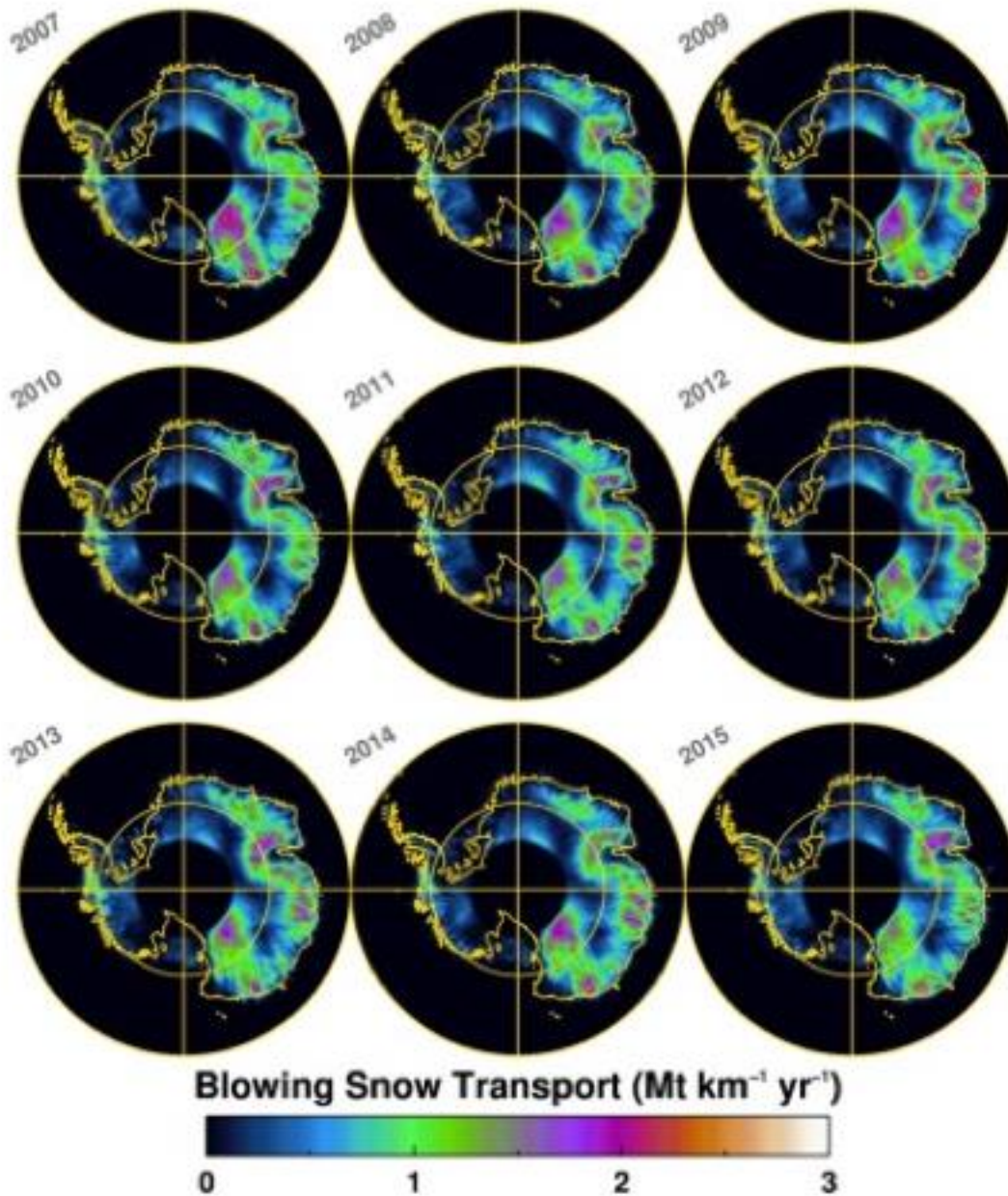
759

760 Figure 8. A large blowing snow storm over Antarctica with blowing snow transport from
 761 continent to ocean on October 14, 2009. (a) CALIOP 532 nm attenuated backscatter along the
 762 yellow (south to north) line bounded by the green arrows as shown in (b) at 06:11 – 06:15 UTC.
 763 (b) MODIS false color image at 06:06:14 – 06:17:31 UTC showing blowing snow as dirty white
 764 areas. The coastline is indicated by the green dots, and two CALIPSO tracks, where blowing
 765 snow was detected are indicated by the yellow lines. (c) CALIOP 532 nm attenuated backscatter
 766 along the yellow (north to south) line, 14:18 – 14:25 UTC.



767

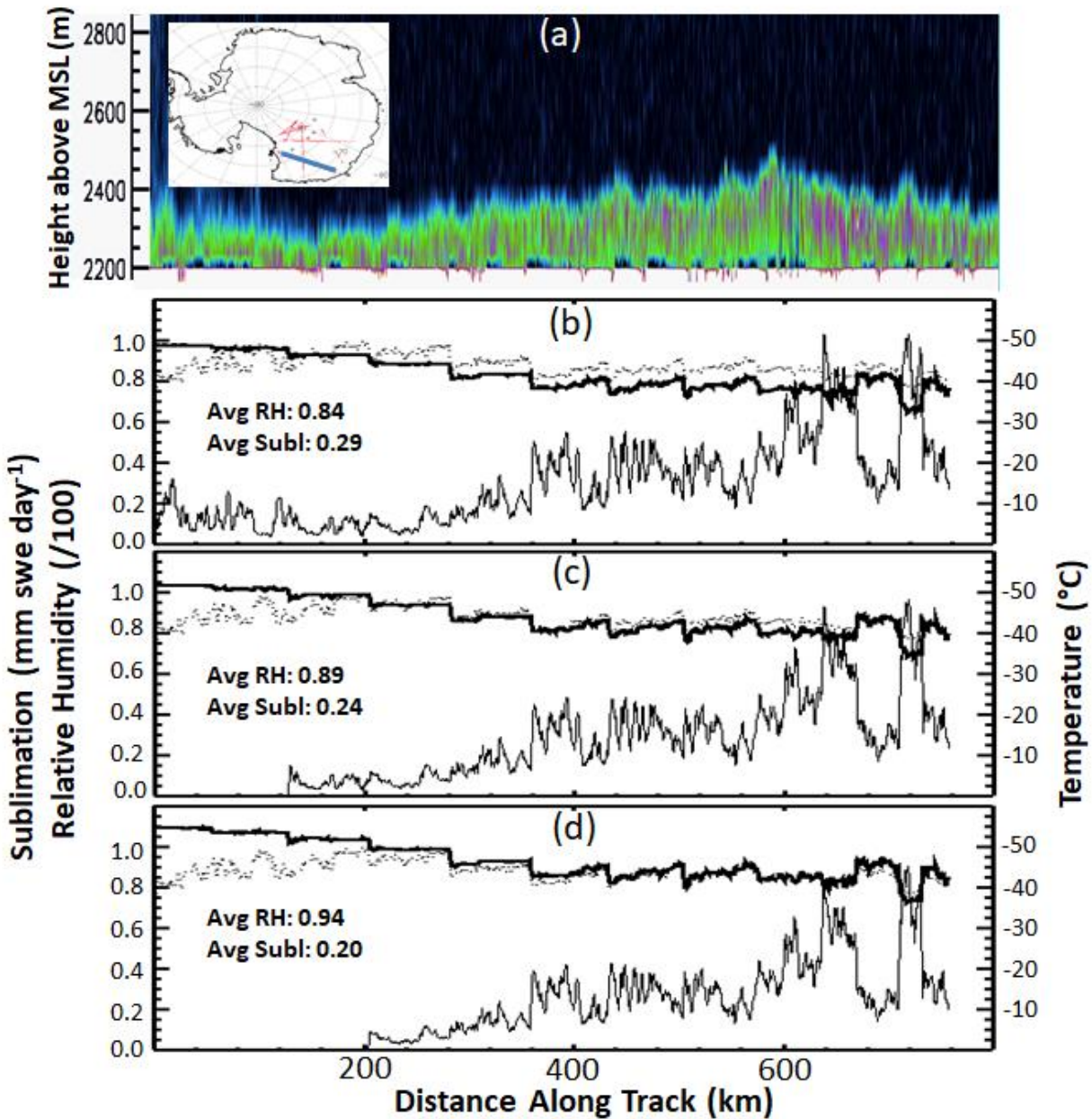
768 Figure 9. (a) MODIS false color image on October 13, 2009, 23:00 UTC and (b) October 14, 2009,
 769 06:16 UTC. The red line is the approximate position of the coastline. (c) The 10 m wind speed
 770 from the AMPS model (Antarctic Mesoscale Prediction System) for October 14, 2009. The area
 771 covered by the MODIS images is roughly that indicated by the blue box in (c).



772

773 Figure 10. The magnitude of blowing snow transport over Antarctica integrated over the year
 774 for years 2007–2015.

775



776

777 Figure 11. (a) CALIPSO backscatter showing blowing snow layer along the blue line in the map
 778 inset on 10/12/2010 at 05:51 UTC. (b) Average MERRA-2 moisture (dark black line),
 779 temperature (dotted line) and calculated sublimation through the blowing snow layer along the
 780 CALIPSO track. (c and d) Same as in (b) but increasing MERRA-2 humidity by 5 and 10%,
 781 respectively.

782